

Adaptive discontinuous Galerkin on polytopic meshes

Andrea Cangiani

SISSA

LMS Research School Adaptive Methods & mOdel Reduction

Nottingham, 15–19 May 2023

Outline

- General meshes & adaptivity: overview and motivation
- Physical-frame (curved) polytopic IP-dG
- Energy norm a posteriori error analysis: allowing polytopic meshes with arbitrary number of possibly very small faces (irregular hanging nodes)
- Adaptive polytopic IP-dG: numerical examples

General mesh FEM approaches

Classical

- Augmented [FE Strang & Fix (1973).]
- Generalised FEM: [Babuska & Osborn, SINUM, 1983], [Babuska & Melenk, CMAME, 1996]
- Composite Finite Elements (CFE) [Hackbusch & Sauter, Numer. Math., 1997]

Recent

- Harmonic FEM & Polygonal FEM [Sukumar & Tabarraei, Int. J. Numer. Methods Eng., 2004]
- BEM-based FEM [Copeland, Langer & Pusch, DDM XVIII, 2009]
- Extended FEM [Fries & Belytschko, Int. J. Numer. Methods Eng., 2010]
- Mimetic Finite Difference (MFD) [Brezzi, Buffa & Lipnikov, M2AN, 2009]
- Virtual Element Method (VEM) [da Veiga, Brezzi, C, Manzini, Marini & Russo, M3AS, 2013]

General mesh FEM approaches

dG

- Agglomerated DG [Bassi, L. Botti, A. Colombo, S. Rebay, Comput. Fluids, 2012]
Composite DG [Antonietti, Giani, Houston, SIAM J. Sci. Comput., 2013]
- *hp*-IPDG [C, Georgoulis & Houston, M3AS, 2014]
- HDG [Cockburn, Gopalakrishnan & Lazarov, SINUM, 2009]
- Weak Galerkin [Wand & Ye, J. Comput. Appl. Math. 2013]
- Hybrid High-Order (HHO) [Di Pietro & Ern, CMAME, 2015]
- Gradient scheme framework [Droniou, Eymard, Gallouet & Herbin, M3AS, 2013]
- Recovered FEM [Georgoulis & Pryer, CMAME, 2018]

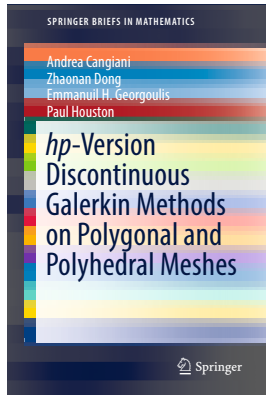
hp -version interior penalty dG method

Preferred approach

Polygonal/polyhedral (**polytopic**) meshes
Interior Penalty discontinuous Galerkin method

[C., Dong, Georgoulis, Houston (SpringerBriefs, 2017)]

- Stable on large class of PDEs
- Flexible hp -version
- Efficient/parallel implementation
- Stable under face/edge degeneration, arbitrary number of faces per element



Generalisation to essentially-arbitrary curved elements

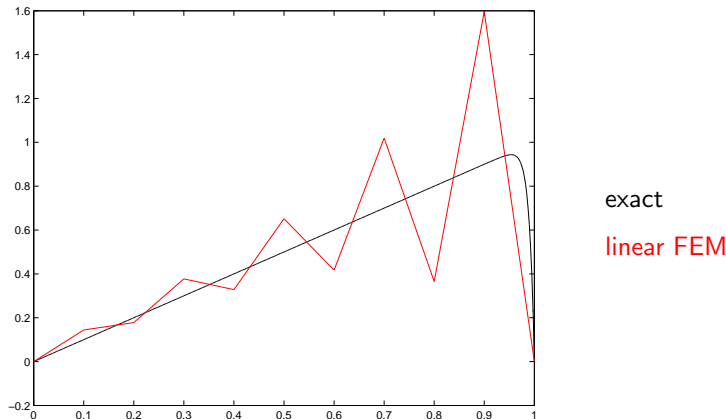
[C., Dong & Georgoulis, Math Comp, 2021]

FEM vs dG...

Consider BVP:

$$\begin{aligned}-\epsilon u''(x) + u'(x) &= 1, \quad x \in (0, 1), \\ u(0) &= 0 = u(1).\end{aligned}$$

Let $\epsilon = 0.01$...

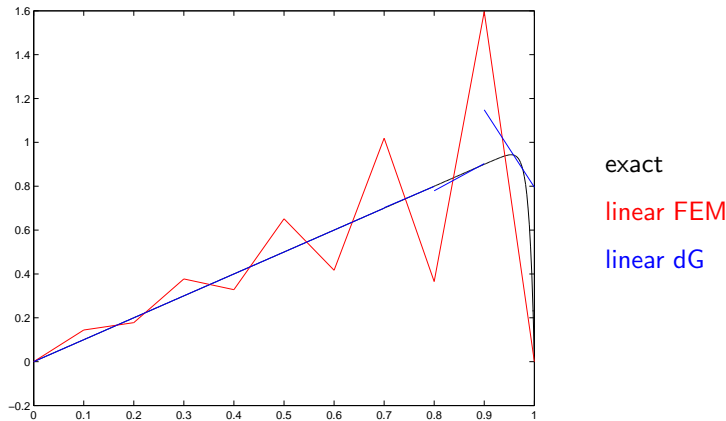


FEM vs dG...

Consider BVP:

$$\begin{aligned}-\epsilon u''(x) + u'(x) &= 1, \quad x \in (0, 1), \\ u(0) &= 0 = u(1).\end{aligned}$$

Let $\epsilon = 0.01$...



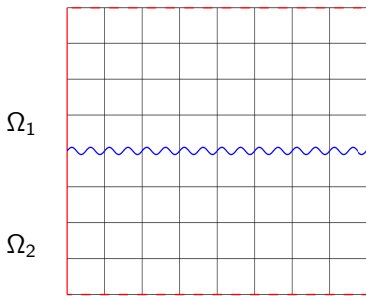
Changing type PDE across a curved interface

(parabolic) $-x_1^2 u_{x_2 x_2} + u_{x_1} + A\omega\pi \cos(\omega\pi x_1)u_{x_2} + u = 0,$ in $\Omega_1,$

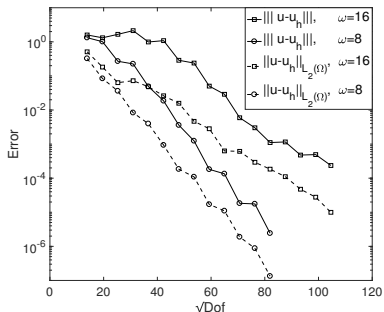
(hyperbolic) $u_{x_1} + A\omega\pi \cos(\omega\pi x_1)u_{x_2} + u = 0,$ in $\Omega_2,$

with $A = 0.025$, and $\omega = 8$ and $\omega = 16.$

The solution is discontinuous across interface.



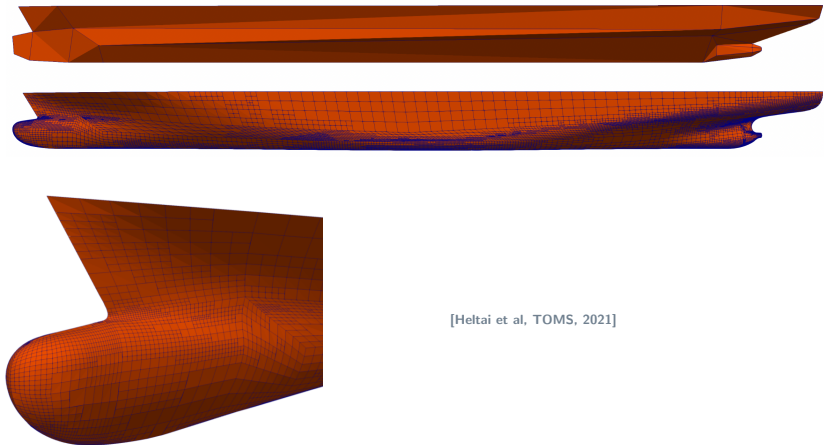
Conforming fixed coarse mesh.



Spectral accuracy.

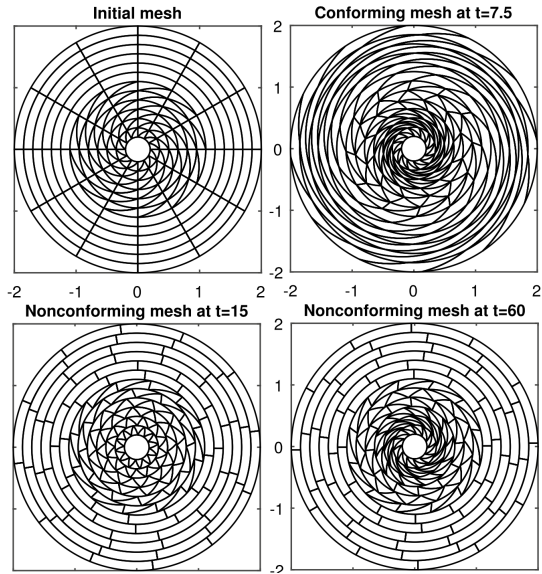
General meshes: exact geometrical model representation

Grids of the Kriso KCS hull.



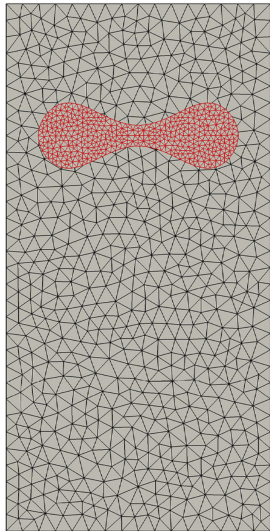
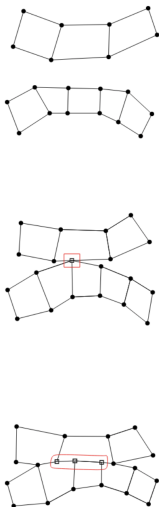
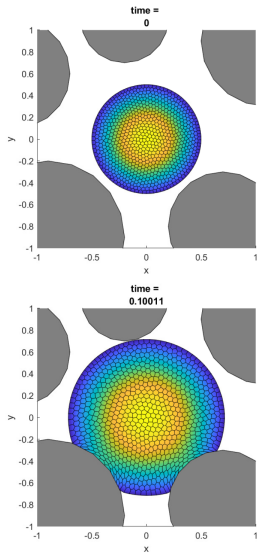
[Heltai et al, TOMS, 2021]

General meshes: naturally arise in Lagrangian approaches



[Gaburro, ACME, 2020]

General meshes: moving objects



[Wells, Hubbard & C., arXiv, 2022]

[Antonietti. et al. (FEAD, 2019)]

Generalisation to essentially-arbitrary curved elements

[C., Dong & Georgoulis, Math Comp, 2021]

- dG with elemental-only DOF (eg. IP, LDG)
 - local dG space independent of element's shape
- Analysis based on new inverse and trace inequalities with no hidden dependence on shape
- Lipschitz elements with general curved interfaces
 - exact representation of curved domains/discontinuity of PDE coefficients
 - spectral accuracy on curved domains without iso-parametric mappings
 - refinement without local re-parametrization

Intro to dG: model problem

On $\Omega \subset \mathbb{R}^d$, bounded open domain with Lipschitz boundary $\partial\Omega$, consider

$$\begin{aligned}-\nabla \cdot (a \nabla u) &= f && \text{in } \Omega, \\ u &= 0 && \text{on } \partial\Omega\end{aligned}$$

$f \in L_2(\Omega)$, $a \in [L_\infty(\Omega)]^{d \times d}$ symmetric and positive.

Weak form: find $u \in V := H_0^1(\Omega)$, such that

$$\int_{\Omega} a \nabla u \cdot \nabla v \, d\mathbf{x} = \int_{\Omega} f v \, d\mathbf{x} \quad \forall v \in V$$

Physical frame discontinuous spaces on polytopic meshes

Physical frame DG space $S_T^p := \{v \in L^2(\Omega) : v|_\kappa \in \mathcal{P}_{p_\kappa}(\kappa), \forall \kappa \in \mathcal{T}_h\}$

- minimal number of degrees of freedom per element
- local space independent of element shape

$$\Gamma = \Gamma_{\text{int}} \cup \partial\Omega$$

On $F = \partial\kappa_i \cap \partial\kappa_j \subset \Gamma_{\text{int}}$

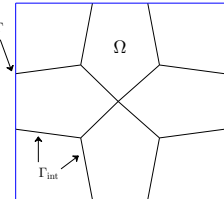
$$\{u\}|_F = \frac{u_{\kappa_i} + u_{\kappa_j}}{2}$$

$$[u]|_F = u_{\kappa_i} \mathbf{n}_{\kappa_i} + u_{\kappa_j} \mathbf{n}_{\kappa_j}$$

On $F = \partial\kappa \subset \partial\Omega$

$$\{u\}|_F = u_{\kappa_i}$$

$$[u]|_F = u_{\kappa_i} \mathbf{n}_{\kappa_i}$$



Magic formula:

$$\sum_{\kappa \in \mathcal{T}} \int_{\partial\kappa} \nabla u \cdot \mathbf{n} \, ds = \int_{\Gamma} \{\nabla v\} \cdot [v] \, ds + \int_{\Gamma_{\text{int}}} [\nabla u] \{v\} \, ds$$

dG derivation

Assume u regular enough and consider $\mathcal{V} = V + S_T^p$ and test with $v \in \mathcal{V}$:

$$-\int_{\Omega} \nabla \cdot (a \nabla u) v \, dx = \int_{\Omega} f v \, dx$$

dG derivation

Assume u regular enough and consider $\mathcal{V} = V + S_T^p$ and test with $v \in \mathcal{V}$:

$$-\sum_{\kappa \in \mathcal{T}} \int_{\kappa} \nabla \cdot (a \nabla u) v \, dx = \int_{\Omega} f v \, dx$$

dG derivation

Assume u regular enough and consider $\mathcal{V} = V + S_T^p$ and test with $v \in \mathcal{V}$:

$$\sum_{\kappa \in T} \int_{\kappa} a \nabla u \cdot \nabla v \, dx - \sum_{\kappa \in T} \int_{\partial \kappa} (a \nabla u \cdot \mathbf{n}_{\kappa}) v \, ds = \int_{\Omega} f v \, dx$$

dG derivation

Assume u regular enough and consider $\mathcal{V} = V + S_T^p$ and test with $v \in \mathcal{V}$:

$$\int_{\Omega} a \nabla_h u \cdot \nabla_h v \, dx - \int_{\Gamma} \{a \nabla u\} \cdot [v] \, ds = \int_{\Omega} fv \, dx$$

To restore symmetry, using $[u] = 0$ add term $[u] \cdot \{a \nabla v\}$

$$\int_{\Omega} a \nabla_h u \cdot \nabla_h v \, dx - \int_{\Gamma} \{a \nabla u\} \cdot [v] \, ds - \int_{\Gamma} [u] \cdot \{a \nabla v\} = \int_{\Omega} fv \, dx$$

Finally, for stability (see later) add term $[u] \cdot [v]$

$$\int_{\Omega} a \nabla_h u \cdot \nabla_h v \, dx - \int_{\Gamma} \{a \nabla u\} \cdot [v] \, ds - \int_{\Gamma} [u] \cdot \{a \nabla v\} + \int_{\Gamma} \sigma[u] \cdot [v] \, ds = \int_{\Omega} fv \, dx$$

for any $\sigma : \Gamma \rightarrow \mathbb{R}^+$ discontinuity penalisation function.

hp -version IP-dG method

dG method: find $u_h \in S_T^p : \mathcal{B}_h(u_h, v) = \ell_h(v)$ for all $v \in S_T^p$

with

$$\mathcal{B}_h(u, v) := \int_{\Omega} a \nabla_h u \cdot \nabla_h v \, dx - \int_{\Gamma} \{a \nabla u\} \cdot [v] \, ds - \int_{\Gamma} [u] \cdot \{a \nabla v\} + \int_{\Gamma} \sigma[u] \cdot [v] \, ds$$

$$\ell_h(v) := \int_{\Omega} fv \, dx$$

Coercivity: for all $v \in S_T^p$,

$$\mathcal{B}_h(v, v) := \int_{\Omega} a \nabla_h v \cdot \nabla_h v \, dx - 2 \int_{\Gamma} \{a \nabla v\} \cdot [v] \, ds + \int_{\Gamma} \sigma[v] \cdot [v] \, ds$$

Introducing dG-norm $\|v\|^2 = \int_{\Omega} a \nabla_h v \cdot \nabla_h v + \int_{\Gamma} \sigma[v] \cdot [v] \, ds$

$$\mathcal{B}_h(v, v) = \|v\|^2 - 2 \int_{\Gamma} \{a \nabla v\} \cdot [v] \, ds$$

Stability by inverse trace estimates

$$\begin{aligned}\mathcal{B}_h(v, v) &= \|v\| - 2 \int_{\Gamma} \{a \nabla v\} \cdot [v] \, ds \\ \Rightarrow \quad \mathcal{B}_h(v, v) &\geq \|v\| - 2 \int_{\Gamma} \sigma^{-1} |\{a \nabla v\}|^2 \, ds - \frac{1}{2} \int_{\Gamma} \sigma |v|^2 \, ds\end{aligned}$$

L^2 -trace inverse estimate: if κ simplex with $h_\kappa := \text{diam}(\kappa)$,

$$\|v\|_{\partial\kappa}^2 \leq C_{\text{inv}} \frac{p^2}{h_\kappa} \|v\|_\kappa^2 \quad \forall v \in \mathcal{P}_p(\kappa)$$

Theorem (Stability)

If $\sigma(x) = C_\sigma \max_{\kappa \in \{\kappa_i, \kappa_j\}} \left\{ \frac{\bar{a}_\kappa C_{\text{inv}}}{h_\kappa} \right\}$, $x \in F \in \Gamma_{\text{int}}$, $F \subseteq \partial\kappa_i \cap \partial\kappa_j$, with $C_\sigma > 0$, then

$$\mathcal{B}_h(v, v) \geq C \|v\| \quad \forall v \in S_T^p$$

What about general (curved) elements???

General curved elements assumptions

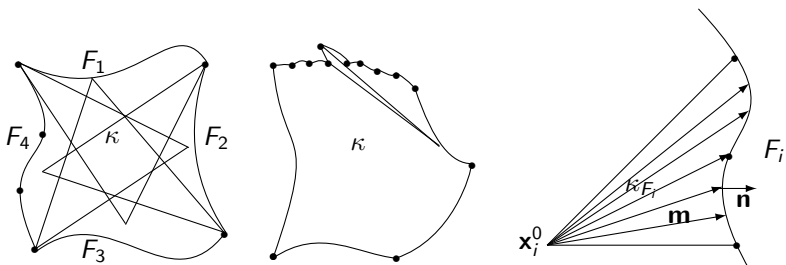
Assumption I: Lipschitz locally star-shaped elements

Each $\kappa \in \mathcal{T}$ is Lipschitz and there exists

- a subdivision of $\partial\kappa$ into mutually exclusive sub-sets $\{F_i\}_{i=1}^{n_\kappa}$, and
- respective generalised simplices $\kappa_{F_i} \subset \kappa$ with $F_i \subset \partial\kappa_{F_i}$ and d planar faces meeting at one point $\mathbf{x}_i^0 \in \kappa$

such that

- (a) each κ_{F_i} is star-shaped with respect to \mathbf{x}_i^0
- (b) $\mathbf{m}(\mathbf{x}) \cdot \mathbf{n}(\mathbf{x}) > 0$ for $\mathbf{x} \in F_i$, with $\mathbf{m}(\mathbf{x}) := \mathbf{x} - \mathbf{x}_i^0$, $\mathbf{x} \in \kappa_{F_i}$

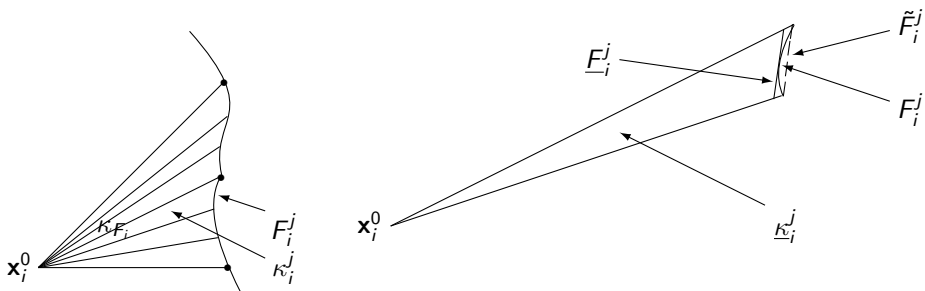


A trace inverse estimate

Lemma

Let element $\kappa \in \mathcal{T}$, satisfying Assumption I. Then, for each $F_i \subset \partial\kappa$, $i = 1, \dots, n_\kappa$, and for each $v \in \mathcal{P}_p(\kappa)$, we have the trace inverse estimate

$$\|v\|_{F_i}^2 \leq \frac{(p+1)(p+d)}{\min_{x \in F_i} (\mathbf{m} \cdot \mathbf{n})} \|v\|_{\kappa_{F_i}}^2$$



Apply trace inverse estimate to curved simplices $\underline{\kappa}_i^j$ and sum up.

A trace inverse estimate

Lemma

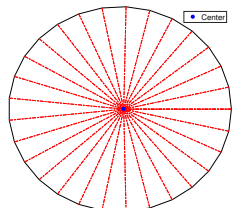
Let element $\kappa \in \mathcal{T}$, satisfying Assumption I. Then, for each $F_i \subset \partial\kappa$, $i = 1, \dots, n_\kappa$, and for each $v \in \mathcal{P}_p(\kappa)$, we have the trace inverse estimate

$$\|v\|_{F_i}^2 \leq \frac{(p+1)(p+d)}{\min_{x \in F_i} (\mathbf{m} \cdot \mathbf{n})} \|v\|_{\kappa_{F_i}}^2$$

- constant depends on \mathbf{x}_i^0 – optimization possible!
- directly extends trace inverse estimates on simplices
- typically, we have $\mathbf{m}(x) \cdot \mathbf{n}(x) \geq c_{sh} h_{\kappa_{F_i}}$, then

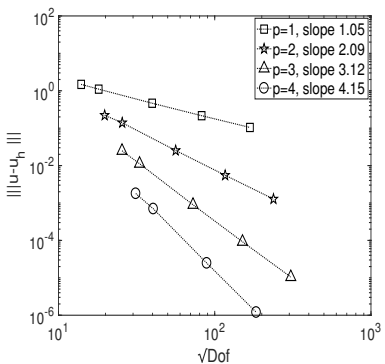
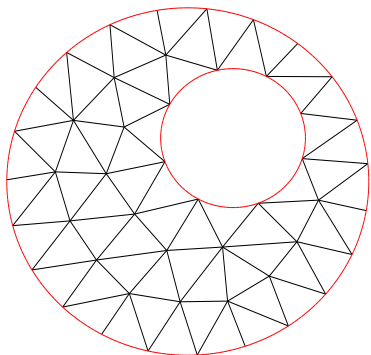
$$\|v\|_{\partial\kappa}^2 \leq Cp^2 h_\kappa^{-1} \|v\|_\kappa^2$$

For κ ball of radius R , $\|v\|_{\partial\kappa}^2 \leq \frac{(p+1)(p+2)}{R} \|v\|_\kappa^2$.



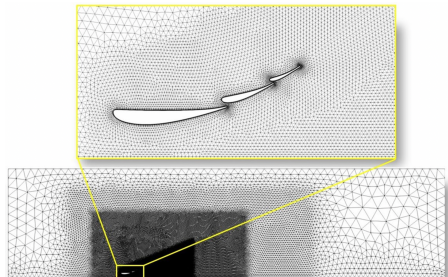
Curved elements

$$-\nabla \cdot (a \nabla u) = f \text{ with } a = 1 \times I_{2 \times 2}, \quad u(x, y) = \sin(\pi x) \sin(\pi y)$$

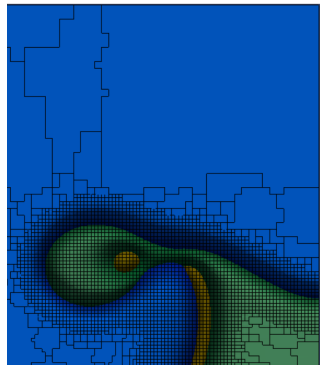


$p = 1, 2, 3, 4$ and 65, 109, 527, 2266, 9411 (curved) elements.

General meshes: adaptivity



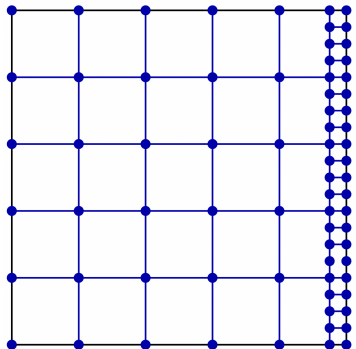
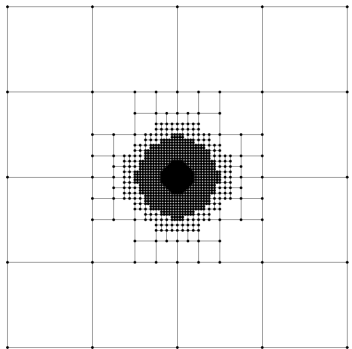
[Slaughter, Moxey & Sherwin, Flow Turbul Combust, 2023]



[Sutton, PhD Thesis, Leicester 2017]

General meshes: adaptivity

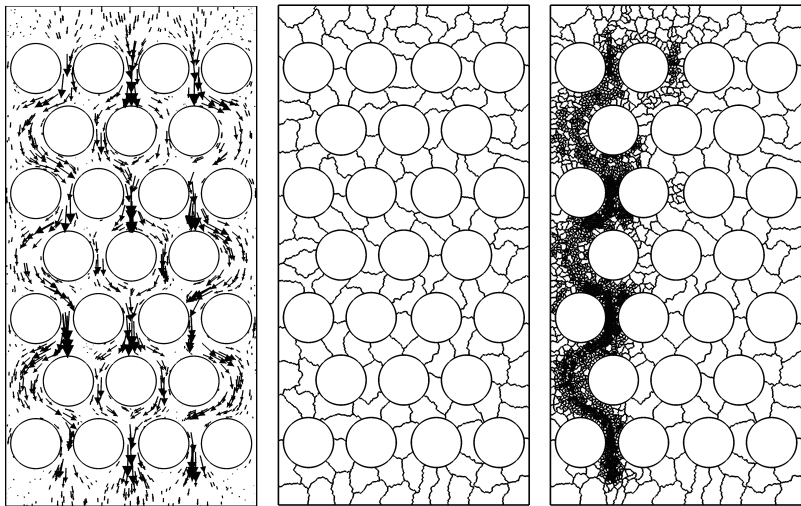
NOTE: standard elements with hanging nodes are polytops!



Adaptive dG (h/hp): modification is fully local.

General meshes: adaptivity

Complicated domains & adaptivity: interstitial flow modelling of drug



Goal-oriented a posteriori error estimation

Let V, W Hilbert with bounded and linear

$$\mathcal{B} : V \times W \rightarrow \mathbb{R}, \quad \ell : W \rightarrow \mathbb{R}$$

and $u \in V$ unique solution of

$$u \in V : \mathcal{B}(u, w) = \ell(w) \quad \forall w \in W.$$

V_h, W_h discrete **subspaces** (!) with

$$\mathcal{B}_h : V \times W \rightarrow \mathbb{R}, \quad \ell_h : W \rightarrow \mathbb{R},$$

providing a **consistent** discretisation

$$u_h \in V_h : \mathcal{B}_h(u_h, w_h) = \ell_h(w_h) \quad \forall w_h \in W_h,$$

so that

$$\mathcal{B}_h(u - u_h, w_h) = 0 \quad \forall w_h \in W_h \quad (\text{Galerkin orthogonality})$$

Let $J(\cdot)$ a linear target functional with $J_h(\cdot)$ consistent reformulation.

Dual-weighted-residual (DWR) a posteriori error analysis

Define adjoint/dual problem

$$z \in W : \mathcal{B}_h(v, z) = J_h(v) \quad \forall v \in V.$$

We have

$$\begin{aligned} J(u) - J_h(u_h) &= J_h(u) - J_h(u_h) = J_h(u - u_h) \\ &= \mathcal{B}_h(u - u_h, z) = \mathcal{B}_h(u - u_h, z - z_h) \\ &= \ell_h(z - z_h) - \mathcal{B}_h(u_h, z - z_h) \quad \forall z_h \in W_h \\ &=: \sum_{\kappa \in \mathcal{T}} \eta_\kappa. \end{aligned}$$

The local error indicators η_κ still depend on the dual solution z .

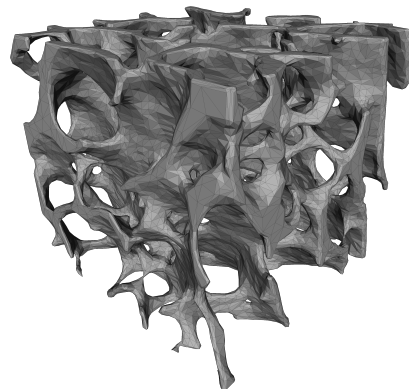
Strategy: approximate it with appropriate $z_{\hat{\kappa}}$ using finer mesh, higher polynomials, or some form of patchwise recovery/reconstruction.

Note! Non-conforming case needs a bit more work....see later in the case of residual-based analysis.

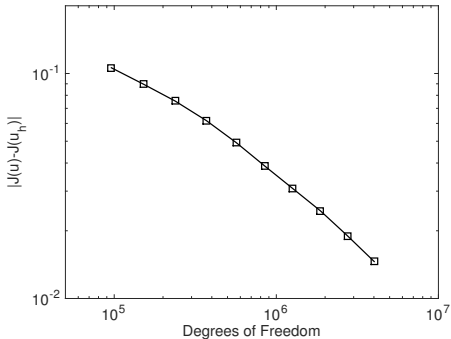
Goal oriented adaptivity on complicated domains

[C, Dong, Georgoulis, Houston, Springer Briefs, 2017]

Linear elastic analysis of a section of trabecular bone



- Model: 1,179,569 tetrahedral elements
- agglomerated to generate a coarse polytopic mesh of 8000 elements
- goal-oriented adaptive algorithm



Convergence of DWR error estimator of Young's modulus

Residual-based a posteriori error estimation and adaptivity

PDE stability + Galerkin orthogonality & Approximation error estimates



Robust and efficient a posteriori¹ error estimation.

- A posteriori bounds used to drive automatic adaptive approaches
- General meshes provide a more flexible tool.

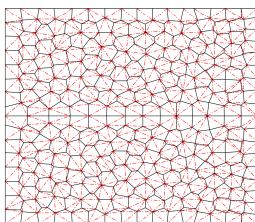
[Giani & Houston 2014, Collins & Houston 2016]

¹A posteriori bounds only depend on computable quantities.

DG FEM a posteriori analysis & adaptivity

General meshes \rightsquigarrow discretisations fitted to geometric model \rightsquigarrow ease of use of PDE stability linking error with the residual

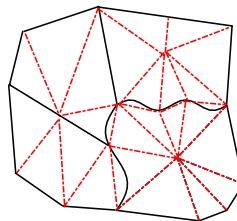
- Unfitted approaches: [Dörfler & Rumpf, Math Comp 1998, Ainsworth & Rankin, Tech Rep 2012]



Analysis on shape-regular polytopic meshes is standard

- by conconforming FEM recovery

[Karakashian & Pascal, SINUM, 2003]



Analysis with generally shaped elements:
NON-TRIVIAL!

- Curved interface problems
[C., Georgoulis & Sabawi, Math. Comp., 2017]
- New recovery for general meshes
[C., Georgoulis & Dong, ArXiv:2208.08685, 2022]

Residual-based a posteriori error bounds

For simplicity, assume $W = V$. Recall

$$u \in V : \mathcal{B}(u, v) = \ell(v) \quad \forall v \in V$$

and discrete problem

$$u_h \in V_h : \mathcal{B}_h(u_h, v_h) = \ell_h(v_h) \quad \forall v_h \in V_h$$

satisfying Galerkin orthogonality (consistency), for $e = u - u_h$,

$$\mathcal{B}_h(e, v_h) = 0 \quad \forall v_h \in V_h$$

Definition (Residual)

The residual $\mathcal{R} \in V'$ is given by

$$\begin{aligned} \langle \mathcal{R}, v \rangle &= \mathcal{R}(v) := \ell_h(v) - \mathcal{B}_h(u_h, v) \quad \forall v \in V \\ &= \mathcal{B}_h(u - u_h, v) = \mathcal{B}_h(e, v), \end{aligned}$$

so that $\|\mathcal{R}\|_{V'} = \sup_{v \in V} \frac{|\langle \mathcal{R}, v \rangle|}{\|v\|_V}$.

Upper and lower bound of the energy error by the residual

Suppose

$$\mathcal{B}_h(v, w) \leq \gamma \|v\|_V \|w\|_V \quad (\text{continuity of } \mathcal{B}_h),$$

and

$$\mathcal{B}_h(v, v) \geq \alpha \|v\|_V^2 \quad (\text{coercivity of } \mathcal{B}_h)$$

we have

$$\alpha \|e\|_V \leq \|\mathcal{R}\|_{V'} \leq \gamma \|e\|_V$$

and it remains to express the residual in terms of computable quantities...

Bound of the residual: Poisson problem $-\Delta u = f$

- $V = H_0^1(\Omega)$ with $\|v\|_V^2 = |v|_{1,\Omega}^2 = (\nabla v, \nabla v)_\Omega$,
- \mathcal{T} simplicial and V_h classical H^1 -conforming FEM
- $\mathcal{B}(u, v) = \mathcal{B}_h(u, v) = (\nabla u, \nabla v)_\Omega$, $\ell(v) = \ell_h(v) = (f, v)_\Omega$.

Then,

$$\begin{aligned}\langle \mathcal{R}, v \rangle &= \mathcal{B}(e, v) = \mathcal{B}(u - u_h, v - v_h) \quad \forall v_h \in V_h \\ &= \ell(v - v_h) - \mathcal{B}(u_h, v - v_h) = \int_\Omega f v - \int_\Omega \nabla u_h \cdot \nabla (v - v_h)\end{aligned}$$

$$= \sum_{\kappa \in \mathcal{T}} \left(\int_\kappa (f + \Delta u_h)(v - v_h) - \sum_{f \in \partial \kappa} \frac{\partial u_h}{\partial \mathbf{n}_f^\kappa} (v - v_h) \right)$$

$$= \sum_{\kappa \in \mathcal{T}} \left(\int_\kappa (f + \Delta u_h)(v - v_h) - \frac{1}{2} \sum_{f \in \partial \kappa} [\![\frac{\partial u_h}{\partial \mathbf{n}}]\!] (v - v_h) \right)$$

$$\Rightarrow |\langle \mathcal{R}, v \rangle| \leq \sum_{\kappa \in \mathcal{T}} \left(\|f + \Delta u_h\|_{0,\kappa} \|v - v_h\|_{0,\kappa} + \frac{1}{2} \|[\![\frac{\partial u_h}{\partial \mathbf{n}}]\!]\|_{0,\partial \kappa} \|v - v_h\|_{0,\partial \kappa} \right)$$

Quasi-interpolation

$$|\langle \mathcal{R}, v \rangle| \leq \sum_{\kappa \in \mathcal{T}} \left(\|f + \Delta u_h\|_{0,\kappa} \|v - v_h\|_{0,\kappa} + \frac{1}{2} \|\llbracket \frac{\partial u_h}{\partial \mathbf{n}} \rrbracket\|_{0,\partial\kappa} \|v - v_h\|_{0,\partial\kappa} \right)$$

- bounding terms do not depend on the exact solution u
- $\forall v \in V$ need v_h so that norms of $v - v_h$ can be bounded in H^1

Theorem (Quasi interpolation)

[Clément, RAIRO, 1975], [Scott & Zhang, Math Comp, 1990], [Bernardi & Girault, SINUM, 1998]

Assume family \mathcal{T} is shape-regular. Then for each $v \in H_0^1(\Omega)$ there exists $I_h v \in V_h$ such that for all $\kappa \in \mathcal{T}$

$$h_\kappa |v - I_h v|_{1,\kappa} + \|v - I_h v\|_{0,\kappa} \leq C_I h_\kappa |v|_{1,\tilde{E}},$$

and

$$\|v - I_h v\|_{0,f} \leq C_I h_\kappa^{1/2} \|v\|_{1,\tilde{E}},$$

where \tilde{E} denotes the patch of elements neighbouring E .

Energy-norm a posteriori error estimate

$$\begin{aligned} |\langle \mathcal{R}, v \rangle| &\leq \sum_{\kappa \in \mathcal{T}} \left(\|f + \Delta u_h\|_{0,\kappa} \|v - v_h\|_{0,\kappa} + \frac{1}{2} \|\llbracket \frac{\partial u_h}{\partial \mathbf{n}} \rrbracket\|_{0,\partial\kappa} \|v - v_h\|_{0,\partial\kappa} \right) \\ &\leq C_I \left[\sum_{\kappa \in \mathcal{T}} \left(\underbrace{h_\kappa \|f + \Delta u_h\|_{0,\kappa} + \frac{1}{2} h_\kappa^{1/2} \|\llbracket \frac{\partial u_h}{\partial \mathbf{n}} \rrbracket\|_{0,\partial\kappa}}_{\eta_\kappa} \right)^2 \right]^{1/2} \left[\sum_{\kappa \in \mathcal{T}} \|v\|_{1,\kappa}^2 \right]^{1/2} \\ &\leq C_I \sqrt{n} \sqrt{1 + C_\Omega^2} \left[\sum_{\kappa \in \mathcal{T}} \eta_\kappa^2 \right]^{1/2} \|v\|_V \end{aligned}$$

with C_Ω^2 the Poincaré constant and as from \mathcal{T} being shape-regular it follows that the number of neighbours is bounded by some n .

$$\Rightarrow \|u - u_h\|_V \leq \frac{1}{\alpha} \|\mathcal{R}\|_{V'} \leq C(C_\Omega, \alpha, C_I, n) \left[\sum_{\kappa \in \mathcal{T}} \eta_\kappa^2 \right]^{1/2}$$

Back to dG: Polytopic mesh assumptions

[C, Dong, Georgoulis & Houston, Springer Briefs, 2017], [C, Dong & Georgoulis, Math. Comp., 2022]]

Mesh sequence: polytopic (polygonal/polyhedral) $\kappa \in \mathcal{T}$.

Mesh skeleton: decomposed into $(d - 1)$ -dimensional simplices $F \in \Gamma$.

There exists $\tau, \rho > 0$ such that:

Domain saturation

- If $\kappa \in \mathcal{T}$ and $F \subset \partial\kappa \cap \partial\Omega$ then $h_F \geq \tau^{-1} h_\kappa$.

Shape-regularity

- $\forall \kappa \in \mathcal{T}$ is (union of) star-shaped wrt a ball of radius $r_\kappa \geq \tau^{-1} h_\kappa$;
- $\forall F \subset \partial\kappa \cap \partial\Omega$ contains a ball of radius $r_F \geq \tau^{-1} h_F$;

Local quasi-uniformity

- If $\kappa_i, \kappa_j \in \mathcal{T}$ share a common interface, then $\rho^{-1} \leq h_{\kappa_i}/h_{\kappa_j} \leq \rho$.

IP-dG method – theoretical trick: inconsistent version

Issue: for u less regular, eg. $u \in H^1(\Omega)$ only, trace of ∇u on Γ not well defined!

IP-dG method: Find $u_h \in S_h^p$: $\mathcal{B}_h(u_h, v) = \ell(v)$ for all $v \in S_h^p$

with

$$\begin{aligned}\mathcal{B}_h(u, v) &= \sum_{K \in \mathcal{T}} \int_K \nabla u \cdot \nabla v \, dx - \int_{\Gamma \setminus \Gamma_N} (\{\Pi \nabla u\} \cdot [\![v]\!] + \{\Pi \nabla v\} \cdot [\![u]\!]) \, ds \\ &\quad + \int_{\Gamma} \sigma [\![u]\!] \cdot [\![v]\!] \, ds \quad \forall u, v \in \mathcal{V} \quad (\text{recall, } \mathcal{V} = V + S_{\mathcal{T}}^p)\end{aligned}$$

$$\ell(v) := \int_{\Omega} fv \, d\mathbf{x} - \int_{\Gamma_D} g_D (a \Pi \nabla v \cdot \mathbf{n} - \sigma v) \, ds + \int_{\Gamma_N} g_N v \, ds$$

with Π the L^2 -orthogonal projection onto $S_{\mathcal{T}}^p$. Now \mathcal{B}_h is stable in \mathcal{V} but inconsistent in that $\mathcal{B}_h(u, v) \neq \ell(v)$.

DG a posteriori error analysis

Error equation. For all $v \in V$ (yes, we can!)

$$\begin{aligned}\mathcal{B}_h(e, v) &= \ell(v) - \mathcal{B}_h(u_h, v) \\ &= \ell(v) - \mathcal{B}_h(u_h, v - v_h) - \mathcal{B}_h(u_h, v_h) \\ &= \ell(\eta) - \mathcal{B}_h(u_h, \eta),\end{aligned}$$

with $\eta := v - v_h$ for any $v_h \in S_T^p$.

Error decomposition. Let $u_c \in V$ some conforming recovery and decompose the error into two components:

$$e = u - u_h = (u - u_c) + (u_c - u_h) =: e_c + e_d.$$

Choosing $v = e_c$ in error equation, we deduce

$$\|e_c\|^2 = \|\sqrt{a} \nabla e_c\|_{\Omega}^2 = \mathcal{B}_h(e_c, e_c) = (\ell(\eta) - \mathcal{B}_h(u_h, \eta)) - \mathcal{B}_h(e_d, e_c).$$

DG a posteriori error analysis (cont.)

Choosing $v_h = \Pi_p e_c \in S_T^p$ appropriately,

$$\begin{aligned} I(\eta) - \mathcal{B}_h(u_h, \eta) &\leq C_1 \left(\sum_{p \in \mathcal{T}} \left(h_p^2 \| (f - \nabla_h(a \nabla_h u_h)) \|_p^2 + h_p \| [a \nabla u_h] \|_{\partial p \cap \Gamma_{\text{int}}}^2 \right. \right. \\ &\quad \left. \left. + \| \sqrt{\sigma}[u_h] \|_{\partial p}^2 \right) \right)^{1/2} \| \sqrt{a} \nabla e_c \| . \end{aligned}$$

For the second term, we have

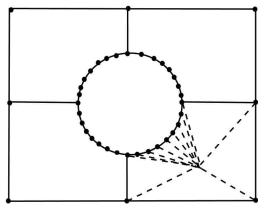
$$|\mathcal{B}_h(e_d, e_c)| \leq C_{\text{cont}} \|e_d\| \|e_c\| = C_{\text{cont}} \|e_d\| \| \sqrt{a} \nabla e_c \| .$$

...and it remains to bound $\| \sqrt{a} \nabla e_d \| ...$

Classical approach: KP (or Oswald) averaging operator

Over a sub-triangulation, use conforming FEM u_c
such that [Karakashian & Pascal (2003)]

$$\|\nabla_h e_d\|^2 \leq \sum_{F \in \Gamma} \|h^{-1/2}[u_h]\|_F^2$$



For \mathcal{T} with small-faces, eg. (multiple) irregular hanging-nodes, resulting bound depends on h_κ/h_F .

Dealing with general interfaces: key ideas

Recovery of dG solution

Given the discrete solution $u_h \in S_T^p$, define the conforming **recovery**^a as the unique $u_c \in H^1(\Omega)$ such that

$$A(u_c, v) = A(u_h, v) \quad \forall v \in H_D^1(\Omega),$$

and $u_c = g_D$ on Γ_D .

^a[Ern & Vohralík (2015), Smears (2018)]

- Essentially independent of the mesh geometry and topology

Helmholtz decomposition

[Dari, Duran, Padra & Vampa M2AN, 1996], [Carstensen, Bartels & Jansche, NM, 2002]

For any $\mathbf{w} \in (L_2(\Omega))^d$, there exists $\xi \in H_0^1(\Omega)$ and $\phi \in [H^1(\Omega)]^{2d-3}$, $d = 2, 3$ such that

$$a\mathbf{w} = a\nabla\xi + \operatorname{curl} \phi \quad \text{in } \Omega,$$

as an orthogonal decomposition and $\|\nabla\phi\| \leq C_\Omega \|\operatorname{curl} \phi\|$.

A posteriori error analysis I

Recall: issue is bound of $\|\sqrt{a}\nabla_h e_d\|$.

Helmholtz decomposition: $a\nabla_h e_d = a\nabla \xi + \operatorname{curl} \phi \Rightarrow \dots \Rightarrow$

$$\|\sqrt{a}\nabla_h e_d\|^2 = \int_{\Omega} a\nabla_h e_d \cdot \nabla \xi d\mathbf{x} + \int_{\Omega} \nabla_h e_d \cdot \operatorname{curl} \phi d\mathbf{x}.$$

Key observation

We only need to control $\phi \in [H^1(\Omega)]^{2d-3} \Rightarrow$ use a “good” mesh!

Auxiliary triangular mesh

Constrained Delaunay Triangulation²: given \mathcal{P} seeds, \mathcal{F} constraints

- if no constraints are given, a CDT is Delaunay
- CDTs maximises the minimum angle

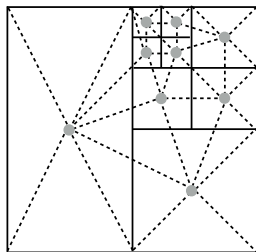
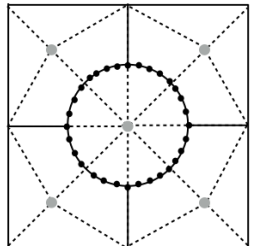
Lemma

There exists a shape-regular Constrained Delaunay Triangulation $\widehat{\mathcal{T}}$ with

- $\mathcal{P} = \{\mathbf{x}_\kappa : \exists \kappa \in \mathcal{T}\}$
 \mathbf{x}_κ := centre of ball inscribed in κ
- $\mathcal{F} = \Gamma \cap \partial\Omega$

such that $\forall T \in \widehat{\mathcal{T}}$ and $\kappa \cap T \neq \emptyset$, $\kappa \in \mathcal{T}$,

$$\widehat{\rho}_2^{-1} \leq h_T/h_\kappa \leq \widehat{\rho}_2.$$



²[Chew (1989), Shewchuk (1998 & 2008)]

A posteriori error estimation

⇒ Apply to ϕ the Scott-Zhang-type quasi-interpolant $I_h\phi$ defined on such auxiliary triangular mesh...

Theorem (Upper bound)

There holds

$$\|u - u_h\| \leq C \left(\sum_{\kappa \in \mathcal{T}} \eta_\kappa^2 \right)^{1/2}$$

with (omitting boundary terms)

$$\begin{aligned} \eta_\kappa^2 = & h_\kappa^2 \| (f - \nabla_h(a \nabla_h u_h)) \|_\kappa^2 + h_\kappa \| [a \nabla u_h] \|_{\partial \kappa \cap \Gamma_{\text{int}}}^2 \\ & + h_\kappa \| [\nabla_T u_h] \|_{\partial \kappa}^2 + \|\sigma^{1/2}[u_h]\|_{\partial \kappa}^2 + O_\kappa^2 \end{aligned}$$

with O_κ collection of standard oscillation terms, and C is independent from h and from the number and measure of the elemental faces.

Why ∇_T ?

The tangential jumps ∇_T in the estimate are desirable.

Remark

On a 'tiny' face $F \subset \Gamma_{\text{int}}$, an inverse estimate yields

$$h_p \|[\nabla_T u_h]\|_F^2 \leq C \frac{h_p}{h_F^2} \| [u_h] \|_F^2$$

i.e., the coefficient becomes unreasonably large when $h_F \ll h_p$.

When, on the other hand, $h_F \sim h_p$, we can have

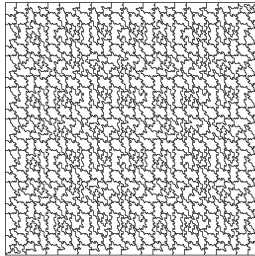
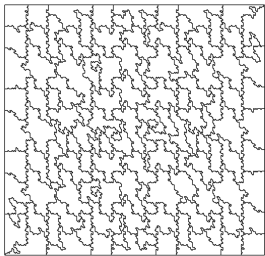
$$h_p \|[\nabla_T u_h]\|_F^2 \leq Ch_p^{-1} \| [u_h] \|_F^2$$

reverting to the familiar residual estimator for IP-dG.

Numerical experiment: influence of tiny faces

Let $a = I_{2 \times 2}$ and $\Omega := (-1, 1)^2$. Solution $u = \sin(\pi x) \sin(\pi y)$.

Sequence of polygonal meshes obtained by successive **agglomeration** of a very fine **triangular background mesh**.



Numerical experiment: influence of tiny faces

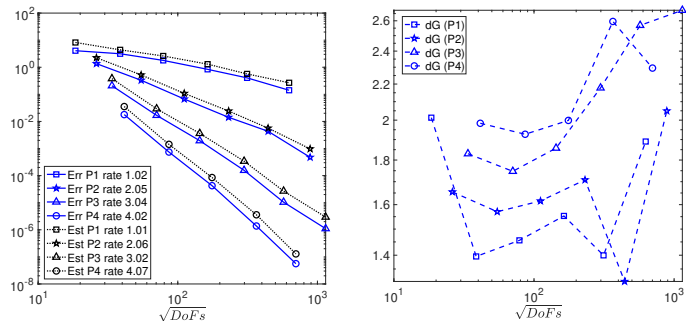


Figure: Example 1. Convergence history of the error and error estimator for $p = 1, 2, 3, 4$ (left) and respective effectivity measured as the ratio estimator over error (right).

Numerical experiment: influences of tiny faces

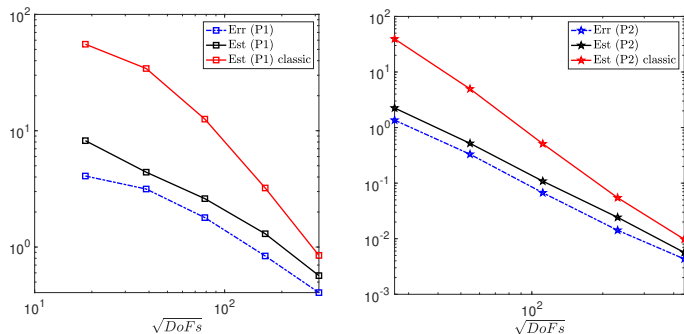


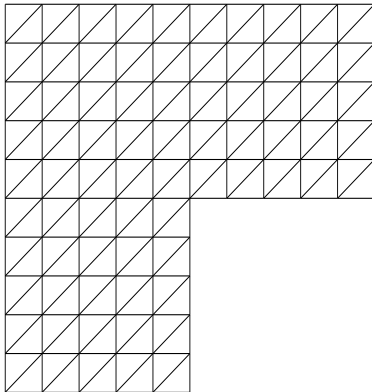
Figure: Example 1. Convergence history of the error, new error estimator and the classical estimator for $p = 1, 2$.

The classical estimator does not contain the tangential gradient jump term, but the jump term depends on the ratio h_p/h_F .

Mesh adaptive coarsening and refinement

$-\nabla \cdot (\textcolor{blue}{a} \nabla u) = f$ with $\textcolor{blue}{a} = 1 \times \textcolor{blue}{I}_{2 \times 2}$ on $\Omega := (-1, 1)^2 \setminus (0, 1) \times (-1, 0)$,

$$u = r^{2/3} \sin(2\psi/3) + \exp(-1000((x - 0.5)^2 + (y - 0.25)^2)) \\ + \exp(-1000((x - 0.5)^2 + (y - 0.75)^2))$$



IP-dG(3) adaptive algorithm:

Dörfler bulk marking:

25% for refinement,

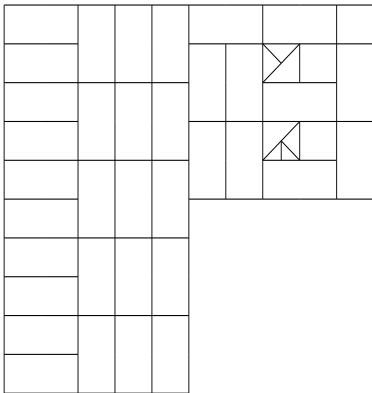
5% for Coarsening

(agglomeration of neighbours
with large sum of jump residuals)

Mesh adaptive coarsening and refinement

$-\nabla \cdot (\textcolor{blue}{a} \nabla u) = f$ with $\textcolor{blue}{a} = 1 \times \textcolor{blue}{I}_{2 \times 2}$ on $\Omega := (-1, 1)^2 \setminus (0, 1) \times (-1, 0)$,

$$u = r^{2/3} \sin(2\psi/3) + \exp(-1000((x - 0.5)^2 + (y - 0.25)^2)) \\ + \exp(-1000((x - 0.5)^2 + (y - 0.75)^2))$$



IP-dG(3) adaptive algorithm:

Dörfler bulk marking:

25% for refinement,

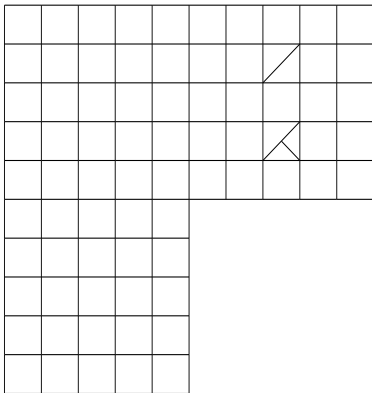
5% for Coarsening

(agglomeration of neighbours
with large sum of jump residuals)

Mesh adaptive coarsening and refinement

$-\nabla \cdot (\textcolor{blue}{a} \nabla u) = f$ with $\textcolor{blue}{a} = 1 \times \textcolor{blue}{I}_{2 \times 2}$ on $\Omega := (-1, 1)^2 \setminus (0, 1) \times (-1, 0)$,

$$u = r^{2/3} \sin(2\psi/3) + \exp(-1000((x - 0.5)^2 + (y - 0.25)^2)) \\ + \exp(-1000((x - 0.5)^2 + (y - 0.75)^2))$$



IP-dG(3) adaptive algorithm:

Dörfler bulk marking:

25% for refinement,

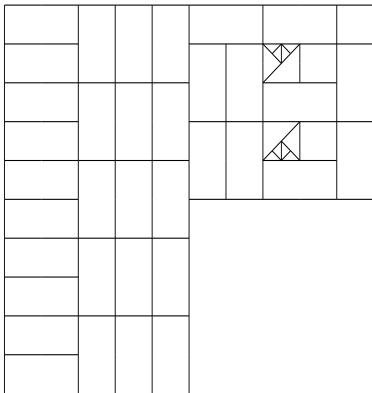
5% for Coarsening

(agglomeration of neighbours
with large sum of jump residuals)

Mesh adaptive coarsening and refinement

$-\nabla \cdot (\textcolor{blue}{a} \nabla u) = f$ with $\textcolor{blue}{a} = 1 \times \textcolor{blue}{I}_{2 \times 2}$ on $\Omega := (-1, 1)^2 \setminus (0, 1) \times (-1, 0)$,

$$u = r^{2/3} \sin(2\psi/3) + \exp(-1000((x - 0.5)^2 + (y - 0.25)^2)) \\ + \exp(-1000((x - 0.5)^2 + (y - 0.75)^2))$$



IP-dG(3) adaptive algorithm:

Dörfler bulk marking:

25% for refinement,

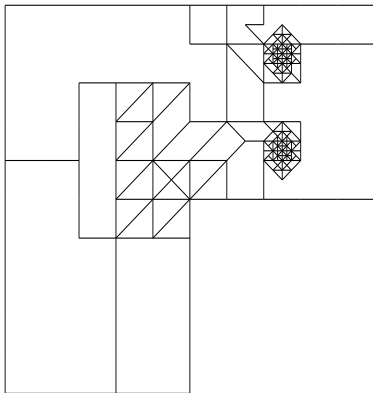
5% for Coarsening

(agglomeration of neighbours
with large sum of jump residuals)

Mesh adaptive coarsening and refinement

$-\nabla \cdot (\textcolor{blue}{a} \nabla u) = f$ with $\textcolor{blue}{a} = 1 \times \textcolor{blue}{I}_{2 \times 2}$ on $\Omega := (-1, 1)^2 \setminus (0, 1) \times (-1, 0)$,

$$u = r^{2/3} \sin(2\psi/3) + \exp(-1000((x - 0.5)^2 + (y - 0.25)^2)) \\ + \exp(-1000((x - 0.5)^2 + (y - 0.75)^2))$$



IP-dG(3) adaptive algorithm:

Dörfler bulk marking:

25% for **refinement**,

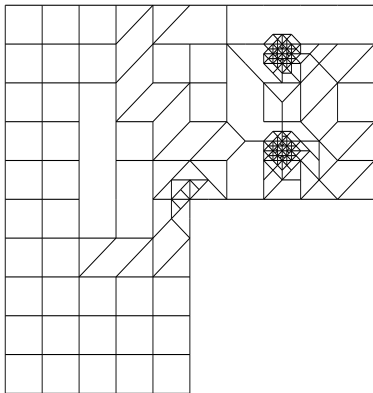
5% for **Coarsening**

(agglomeration of neighbours
with large sum of jump residuals)

Mesh adaptive coarsening and refinement

$-\nabla \cdot (\textcolor{blue}{a} \nabla u) = f$ with $\textcolor{blue}{a} = 1 \times \textcolor{blue}{I}_{2 \times 2}$ on $\Omega := (-1, 1)^2 \setminus (0, 1) \times (-1, 0)$,

$$u = r^{2/3} \sin(2\psi/3) + \exp(-1000((x - 0.5)^2 + (y - 0.25)^2)) \\ + \exp(-1000((x - 0.5)^2 + (y - 0.75)^2))$$



IP-dG(3) adaptive algorithm:

Dörfler bulk marking:

25% for refinement,

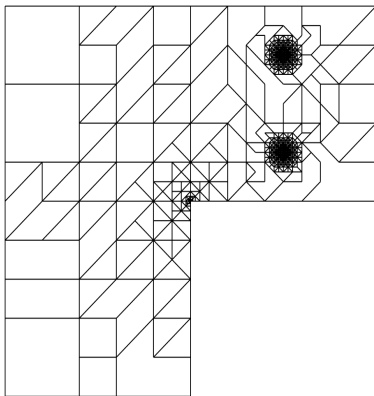
5% for Coarsening

(agglomeration of neighbours
with large sum of jump residuals)

Mesh adaptive coarsening and refinement

$-\nabla \cdot (\textcolor{blue}{a} \nabla u) = f$ with $\textcolor{blue}{a} = 1 \times \mathbf{I}_{2 \times 2}$ on $\Omega := (-1, 1)^2 \setminus (0, 1) \times (-1, 0)$,

$$u = r^{2/3} \sin(2\psi/3) + \exp(-1000((x - 0.5)^2 + (y - 0.25)^2)) \\ + \exp(-1000((x - 0.5)^2 + (y - 0.75)^2))$$



IP-dG(3) adaptive algorithm:

Dörfler bulk marking:

25% for refinement,

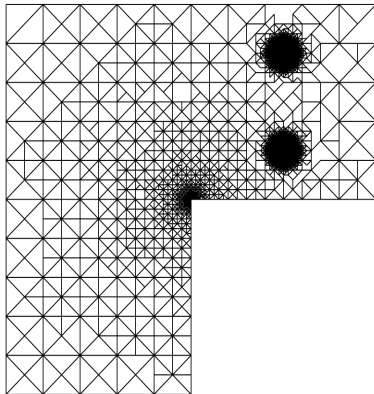
5% for Coarsening

(agglomeration of neighbours
with large sum of jump residuals)

Mesh adaptive coarsening and refinement

$-\nabla \cdot (\textcolor{blue}{a} \nabla u) = f$ with $\textcolor{blue}{a} = 1 \times \mathbf{I}_{2 \times 2}$ on $\Omega := (-1, 1)^2 \setminus (0, 1) \times (-1, 0)$,

$$u = r^{2/3} \sin(2\psi/3) + \exp(-1000((x - 0.5)^2 + (y - 0.25)^2)) \\ + \exp(-1000((x - 0.5)^2 + (y - 0.75)^2))$$



IP-dG(3) adaptive algorithm:
Dörfler bulk marking:
25% for **refinement**,
5% for **Coarsening**
(agglomeration of neighbours
with large sum of jump residuals)

Convergence history

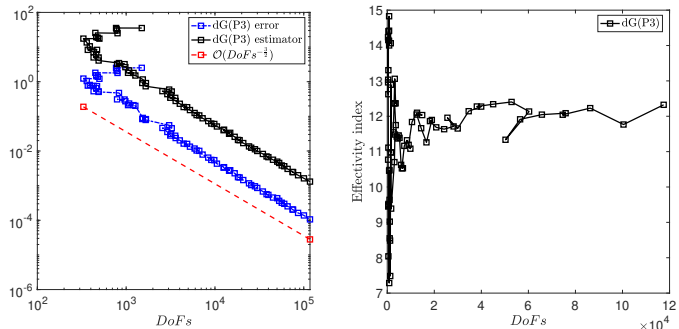


Figure: Error and estimator of the new adaptive polytopic dG method and adaptive dG method without agglomeration for $p = 3$.

Coarsening appears to be improving on the error per DoFs!

More research on algorithms is needed to achieve more significant improvement.

Convergence history

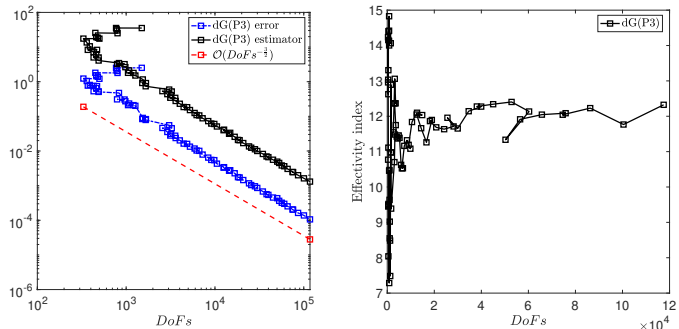


Figure: Error and estimator of the new adaptive polytopic dG method and adaptive dG method without agglomeration for $p = 3$.

Coarsening appears to be improving on the error per DoFs!

More research on algorithms is needed to achieve more significant improvement.

Convergence history

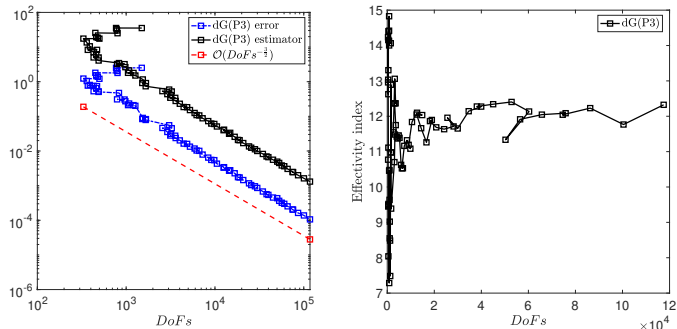


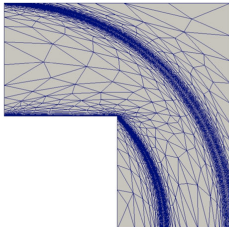
Figure: Error and estimator of the new adaptive polytopic dG method and adaptive dG method without agglomeration for $p = 3$.

Coarsening appears to be improving on the error per DoFs!

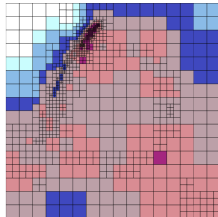
More research on algorithms is needed to achieve more significant improvement.

Conclusions

- A priori analysis of dG for large class of linear PDEs on general curved meshes
- Optimal a posteriori error estimator on very general polytopic meshes
- Extends standard meshes analysis to include multiple irregular hanging nodes.
- Opens wide possibilities within mesh adaptive algorithms, including anisotropic and hp -adaptivity



[Ferro, Perotto, & C., JSciComp, 2022]



[Houston & Süli, SISC, 2001]